Pergamon

PII: S0306-4522(00)00366-3

www.elsevier.com/locate/neuroscience

Neuroscience Vol. 101, No. 2, pp. 323–336, 2000

0306-4522/00 $20.00+0.00

DIFFERENCES IN AMPLITUDE–VOLTAGE RELATIONS BETWEEN MINIMAL AND COMPOSITE MOSSY FIBRE RESPONSES OF RAT CA3 HIPPOCAMPAL NEURONS SUPPORT THE EXISTENCE OF INTRASYNAPTIC EPHAPTIC FEEDBACK IN LARGE SYNAPSES

A. M. KASYANOV,*† V. V. MAXIMOV,‡ A. L. BYZOV,‡ N. BERRETTA,§ M. V. SOKOLOV,‖ S. GASPARINI,§ E. CHERUBINI,§ K. G. REYMANN* and L. L. VORONIN‖¶

*Institute of Higher Nervous Activity and Neurophysiology, Russian Academy of Sciences, 117865 Moscow, Russia

†Leibniz Institute for Neurobiology, 39008 Magdeburg, Germany

‡Institute of Problems of Information Transmission, Russian Academy of Sciences, 104447 Moscow, Russia

§Biophysics Sector and INFM Unit, International School for Advanced Studies, 34014 Trieste, Italy

‖Brain Research Institute, Russian Academy of Medical Sciences, per. Obukha 5, 103064 Moscow, Russia

Abstract—Computer simulations and electrophysiological experiments have been performed to test the hypothesis on the existence of an ephaptic interaction in purely chemical synapses. According to this hypothesis, the excitatory postsynaptic current would depolarize the presynaptic release site and further increase transmitter release, thus creating an intrasynaptic positive feedback. For synapses with the ephaptic feedback, computer simulations predicted non-linear amplitude–voltage relations and voltage dependence of paired-pulse facilitation. The deviation from linearity depended on the strength of the feedback determined by the value of the synaptic cleft resistance. The simulations showed that, in the presence of the intrasynaptic feedback, recruitment of imperfectly clamped synapses and synapses with linear amplitude–voltage relations tended to reduce the non-linearity and voltage dependence of paired-pulse facilitation. Therefore, the simulations predicted that the intrasynaptic feedback would particularly affect small excitatory postsynaptic currents induced by activation of electrotonically close synapses with long synaptic clefts. In electrophysiological experiments performed on hippocampal slices, the whole-cell configuration of the patch-clamp technique was used to record excitatory postsynaptic currents evoked in CA3 pyramidal cells by activation of large mossy fibre synapses. In accordance with the simulation results, minimal excitatory postsynaptic currents exhibited "supralinear" amplitude–voltage relations at hyperpolarized membrane potentials, decreases in the failure rate and voltage-dependent paired-pulse facilitation. Composite excitatory postsynaptic currents evoked by activation of a large amount of presynaptic fibres typically bear linear amplitude–voltage relationships and voltage-independent paired-pulse facilitation.

These data are consistent with the hypothesis on a strong ephaptic feedback in large mossy fibre synapses. The feedback would provide a mechanism whereby signals from large synapses would be amplified. The ephaptic feedback would be more effective on synapses activated in isolation or together with electrotonically remote inputs. During synchronous activation of a large number of neighbouring inputs, suppression of the positive intrasynaptic feedback would prevent abnormal boosting of potent signals.

Key words: excitatory postsynaptic currents, hippocampus, membrane hyperpolarization.

According to the classical view, chemical synaptic transmission is "polarized" in the sense that the signal is passing from the presynaptic to the postsynaptic site. However, chemical "retrograde" signalling has also been suggested whereby postsynaptic events can control presynaptic ones.[49,65] Byzov has hypothesized that a positive intrasynaptic electrical (or ephaptic) feedback can be generated by the excitatory postsynaptic current (EPSC) itself and can increase release probability, thus acting as a retrograde signal.[8,9,40,60] The increase might be caused by the depolarization of the release sites, provided that the resistance of the synaptic cleft is high enough. This would create a positive feedback so that any small increase in EPSC amplitude would be amplified. Therefore, one method to test this hypothesis is to increase the EPSC amplitude in a predictable way and to measure the actual increase. Postsynaptic hyperpolarization is a known reliable method to increase EPSC amplitude. In the presence of any positive ephaptic feedback, the hyperpolarization should increase the amplitude not linearly as a result of the increased driving force for cations,[29] but "supralinearly", due to additional concomitant enhancement of transmitter release. While, in support of this hypothesis, it has recently been shown that artificial postsynaptic hyperpolarization can influence several indices of transmitter release such as the failure rate, the mean quantal content and the coefficient of variation of response amplitude (CV) in a subset of visual cortex and hippocampal CA1 neurons,[61] no deviation from linear amplitude–voltage

¶To whom correspondence should be addressed. Tel.: +7-095-9179664; fax: +7-095-9170595.

E-mail address: brainres@dataforce.net (L. L. Voronin).

Abbreviations: ACSF, artificial cerebrospinal fluid; *A–V*, amplitude–voltage; CF, commissural-associative fibre; CV, coefficient of variation of response amplitude; EGTA, ethyleneglycolbis(aminoethyl ether)tetraacetate; EPSC, excitatory postsynaptic current; EPSC1 and EPSC2, EPSCs evoked by the first and second paired pulses, respectively; EPSP, excitatory postsynaptic potential; HEPES, *N*-2-hydroxyethylpiperazine-*N*′-2-ethanesulphonic acid; I_s, EPSC amplitude; *k*, coefficient of EPSC attenuation along dendrites; *K*, coefficient of intrasynaptic feedback; L-CCG-I, (2*S*,3*s*,4*S*)-CCG/(2*s*,1′*S*,2′*S*)-2-(carboxycyclopropyl)-glycine; MF, mossy fibre; mGluR, metabotropic glutamate receptor; MP, membrane potential; *n*, number of synapses; *N*, sample size; N_0, number of response failures; PPF, paired-pulse facilitation; R_d, dendritic resistance between synapses; R_e, extracellular resistance; R_g, synaptic cleft (gap) resistance; R_s, resistance of the activated subsynaptic membrane; *V*, postsynaptic potential; VDCC, voltage-dependent Ca^{2+} channel; V_g, potential across R_g; V_p, presynaptic potential.

($A-V$) relations has been reported for responses recorded from various structures, including hippocampal areas.[3,21,27] Moreover, recordings of hippocampal α-amino-3-hydroxy-5-methyl-4-isoxazolepropionate-type glutamate receptor-mediated EPSCs at two different membrane potentials (MPs) have revealed no differences[38] in CV or in the paired-pulse facilitation (PPF) ratio,[12,38] which is a known index of presynaptic function.[68] To solve this apparent contradiction, in the present work a computer model, based on different numbers of activated synapses having different magnitudes of intrasynaptic feedback, has been developed. Predictions from the model have been tested in electrophysiological experiments. According to the hypothesis, a membrane hyperpolarization should particularly influence large synapses with long synaptic clefts located in the proximal portion of the apical dendrites, such as the mossy fibre (MF) terminals in the CA3 region of the hippocampus.[11,45] Therefore, we induced EPSCs by MF stimulation. Computer simulations have demonstrated that recruitment of additional synapses tends to linearize $A-V$ relations and to reduce the voltage dependence of PPF. Compatible with the existence of the ephaptic feedback at the MF synapses and its relief with synchronous activation of numerous inputs, physiological experiments showed that minimal MF EPSCs bear a supralinear $A-V$ relation, whereas compound EPSCs elicited by synchronous activation of a large number of presynaptic fibres have a conventional linear $A-V$ relation and smaller (if any) PPF voltage dependence.

EXPERIMENTAL PROCEDURES

Slice preparation and recordings

Experiments were performed on juvenile Wistar rats (from 18 days to six weeks) bred at the Leibniz Institute of Neurobiology, Magdeburg, Brain Research Institute, Moscow or Trieste University, Trieste. All efforts were made to minimize the number of animal used and their suffering. All experiments in Magdeburg and Trieste were carried out in accordance with the European Communities Council Directive of 24 November 1986 (86/609EEC) and in Moscow according to the National Institutes of Health Guide for the Care and Use of Laboratory Animals (NIH Publication No. 80-23) and were approved by the local authority veterinary service. Hippocampal slices were prepared according to the methods already described.[5,51] In brief, animals were decapitated after being anaesthetized with intraperitoneal injection of urethane (2 g/kg). The brain was quickly removed from the skull and the hippocampi were dissected free. Transverse 400- to 600-μm-thick slices were cut with a tissue chopper or with a vibroslicer and maintained at room temperature (22–24°C) in oxygenated artificial cerebrospinal fluid (ACSF) containing (in mM): NaCl 124, KCl 1.5, $CaCl_2$ 2.45, $MgCl_2$ 1.3, KH_2PO_4 1.25, $NaHCO_3$ 25, D-glucose 10. After incubation in ACSF for at least 1 h, an individual slice was transferred to a submerged recording chamber, continuously superfused at 32–33°C with oxygenated ACSF at a rate of 3 ml/min. Picrotoxin (50 μM) and CsCl (2 mM) were routinely added to ACSF in order to block $GABA_A$ receptors and to eliminate possible influences of the hyperpolarization-activated cation current (I_h) on the recorded response.[42] Tetrodotoxin (10 nM) was also present to diminish polysynaptic activation and prevent epileptiform discharges. In four experiments, α-3-(2-carboxy-piperazin-4-yl)-propyl-1-phosphonic acid (20 μM) or D-2-amino-5-phosphonopentanoic acid (50 μM; Cambridge Research Biochemicals) was also added to the extracellular solution to block *N*-methyl-D-aspartate-type receptors. Recording pipettes, pulled from 2-mm borosilicate glass, had a resistance of 2–5 MΩ when filled with an intracellular solution containing (in mM): caesium methanesulphonate 140, $MgCl_2$ 2, HEPES 10, glucose 20, EGTA 0.2. In most experiments, QX-314 (5–10 mM) was added to block voltage-dependent Na^+ conductances. EPSCs were recorded from CA3 pyramidal cells, using the whole-cell configuration of the patch-clamp technique. Recordings were performed after capacitance optimization and series resistance compensation with standard patch-clamp amplifiers (either Axoclamp 2A, Axon Instruments, Foster City, CA, USA or EPC-7, List Medical Instruments, Darmstadt, Germany). Series resistance (typically 10–30 MΩ) and membrane input resistance were estimated by analysing current transients during 3- to 5-mV, 100-ms voltage pulses. The absence of systematic significant changes in the current at different MPs suggested that, in our conditions, the hyperpolarization-activated cation current I_h was largely blocked.[42] Afferent fibres were stimulated with patch pipettes (about 10 μm diameter) filled with ACSF or with bipolar twisted NiCr insulated electrodes (50 μm diameter). The stimulating electrode was placed in the stratum lucidum (see MF-I in Fig. 3A) to stimulate the MF tract. In some experiments, an additional stimulating electrode was used to activate either MF or commissural-associative fibre (CF) input (Fig. 3A). Due to the complexity of the dentate gyrus–CA3 circuitry,[11] isolated activation of the MF input is problematic. In order to see whether the recorded EPSCs really reflected MF activation, in four experiments a selective agonist of the metabotropic glutamate receptors (mGluRs) of group II, (2*S*,3*s*,4*S*)-CCG/(2*s*,1′*S*,2′*S*)-2-(carboxycyclopropyl)glycine (L-CCG-I, 10 μM; Tocris Cookson Ltd., UK), was applied. These receptors are localized only on MFs, and it has been shown that mGluR activation reduces the MF but not the CF responses.[48] As expected, L-CCG-I diminished EPSC amplitude by 40 ± 26% (mean ± S.D., $N=4$; Fig. 7B). These observations indicate that the electrodes shown in Fig. 3A indeed stimulated MFs, but they do not demonstrate that only MFs were activated. We suggest that when composite responses were recorded, mixed MF and non-MF inputs could be activated. Single or paired (50-ms) stimuli (1–10 V, 40–100 μs duration) were delivered every 8 or 15 s and were adjusted either to induce minimal EPSCs with occasional failures or composite EPSCs without failures. As already reported,[61] the effects of MP shifts were not cell- but input-specific. Therefore, the description refers to "inputs" (or EPSCs) rather than "cells".

Experimental protocol

EPSCs were recorded at different holding potentials, starting from "rest" (usually from −60 to −65 mV). Typically, eight to 20 samples were collected at each MP and averaged. To control for stability, responses were repeatedly evoked at the resting MP during the experiment. Recordings with unstable EPSCs at control were rejected. The $A-V$ plots for minimal EPSCs appeared to be less stable than for composite EPSCs. This could be due to (i) response rundown, especially during the initial part of the experiment, which might be explained either by low-frequency depression[28,58] or by stabilization of recording conditions, or both, and (ii) transient or persistent EPSC potentiation.[7] While only one of 15 composite EPSCs recorded at various MPs was rejected because of significant instability, only 12 of 20 recordings of minimal EPSCs from eight of 10 neurons were stable enough to collect four to seven data points for $A-V$ curves. Seven EPSCs evoked by minimal stimulation of the MF input and two EPSCs evoked by minimal stimulation of the CF input were recorded at two different MPs with a different protocol, similar to that used previously in the visual cortex and in hippocampal CA1 neurons.[61] After response stabilization, 75–100 consecutive responses were recorded at −50 or −63 mV. Subsequently, the cell was hyperpolarized by 30 mV (i.e. to −80 or −93 mV) and a further 90–150 responses were collected. The responses were filtered at 1, 3 or 10 kHz, digitized at 5 or 10 kHz and stored on the disc.

Response measurements

The amplitude of composite EPSCs was measured from averaged responses between the poststimulus baseline and the peak. As has been pointed out,[38] in spite of the presence of an Na^+ channel blocker in the recording pipette, signs of voltage-dependent activity appeared in some cases at MPs between −63 and 0 mV, especially in the response to the second pulse in the paired-pulse paradigm. An example is shown in Fig. 3B (−63 mV, response to the second pulse). We tried to choose stimulus parameters that did not trigger such activity and measurement points that did not include it. We note that at hyperpolarized (more negative than −63 mV) and at positive MPs such activity was absent (Fig. 3B, +40 and −109 mV), so that it did not strongly influence the resulting $A-V$ plots.

Measurements of minimal excitatory postsynaptic current and component analysis

To improve the signal-to-noise ratio for minimal EPSCs, we used a

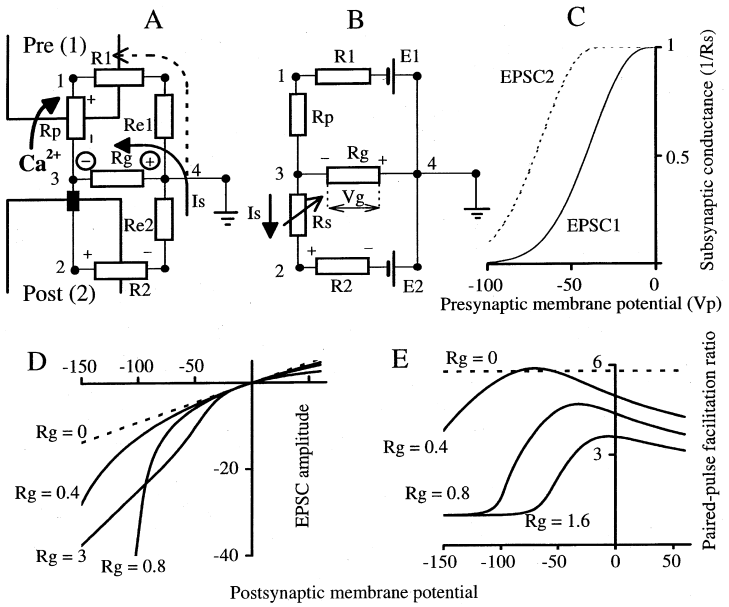

Fig. 1. Basic module of the simulation experiments: chemical synapse with intrasynaptic ephaptic feedback. (A) Presynaptic [Pre (1)] and postsynaptic [Post (2)] cells with respective input resistances (R_1 and R_2). The local resistance of the presynaptic ending at the site of transmitter release is represented separately as R_p. Continuous arrow I_s shows the EPSC generated by opening of respective ionic channels (black box under point 3). The current I_s depolarizes the postsynaptic membrane (+ and − over R_2) and also creates a potential drop V_g over the synaptic cleft resistance (− and + in circles over R_g), which is negative at point 3 relative to the extracellular space (point 4). This negative potential should depolarize the presynaptic membrane close to the locus of transmitter release. This may increase Ca^{2+} influx (left-hand arrow) and transmitter release, and therefore create a positive intrasynaptic feedback. The dashed arrow shows a component of I_s passing through the presynaptic part to give another (but physically equivalent) illustration of the feedback. This component would depolarize the transmitter release site (+ and − over R_p). Note that this component produces a hyperpolarization of the presynaptic part remote from the transmitter release zone and can increase presynaptic spike amplitude here. The resistances of the extracellular space (R_{e1} and R_{e2}) are given to complete the circuit, but they are significantly smaller than all other resistances and can be neglected (see B). (B) Equivalent electrical scheme also showing resting membrane potentials (E_1 and E_2), subsynaptic resistance (R_s) controlled by synaptic transmitter, and potential drop (V_g) generated by I_s across R_g. (C) Dependence of the subsynaptic conductance ($1/R_s$) on the presynaptic membrane potential V_p (continuous curve, EPSC1) used in simulation experiments. To imitate PPF, similar dependence for the second response in the paired-pulse paradigm (EPSC2) was obtained by lateral parallel shift (dashed curve). (D) $A–V$ relationships for various synaptic cleft resistances (R_g). Note the deviation from linearity for $R_g > 0$. The deviation is essential even at resting MP of about −70 mV, when R_g is large enough. Note also a rectification at positive potentials clearly seen for the largest $R_g = 3$ GΩ. Here and in E, the dashed lines represent data for the simulation of synapses without ephaptic feedback ($R_g = 0$). (E) Voltage dependencies of the PPF ratio at various R_g. The PPF ratio is voltage independent in the absence of the ephaptic feedback ($R_g = 0$), whereas in its presence ($R_g > 0$) the shape of the respective function and especially the location of its maximum depend on the R_g value. The point at 0 mV was not calculated because it is a ratio of zero to zero. Here and in Fig. 2, the dimensions are not given because they are conventional units used in simulations, but they can be taken as gigaohms for the resistances and millivolts for the potentials.

covariance measure provided by the multivariate techniques of the principal component analysis.[25] Its application to the minimal synaptic responses has recently been described in detail.[2] In brief, scores of the first principal component were determined from the initial slope and the peak using an algorithm written on the basis of the standard principal component analysis.[25] Such integral "covariance amplitudes" were strongly correlated with more common measures of peak amplitudes. They were recalculated into pA using comparison of peak amplitudes and scores of averaged waveforms, and they are referred to in the text as "amplitudes" for simplicity. For four minimal EPSCs, we compared $A–V$ curves obtained by measuring conventional peak amplitudes from averages with the mean values calculated from the respective component scores. The $A–V$ curves were not significantly different. In addition, a special algorithm[2] was used to separate components of minimal EPSCs having different latencies and kinetics, and therefore mediated by different inputs. Applications of this algorithm to minimal hippocampal responses have been described recently.[2,5,61] The component analysis was performed here for six of nine minimal EPSCs which were used for construction of $A–V$ relations and had enough statistics for reliable analysis ($N > 200$ trials). There were four cases with two components and one case with three components. The different latency and kinetics strongly suggested that the separated components were mediated by different inputs, i.e. by different axons or synapses.[2] These procedures allowed us not only to increase the signal-to noise ratio, but also to make more precise analysis separating individual inputs from mixed minimal EPSCs. It also increased the sample size, which was important because obtaining $A–V$ curves under stable recording conditions is not easy. Data are expressed as means ± S.E.M. unless stated otherwise. Differences were evaluated with Student's t-test for paired data, and $P < 0.05$ was considered as statistically significant.

Estimation of the number of response failures

To estimate the number of response failures (N_0) from recordings of minimal EPSCs we used two methods.[58] Firstly, we separated failures from successes visually (Fig. 6B, C). Averaging of failures was used to control the separation.[28] Secondly, we estimated N_0 as the double number of positive amplitudes. The similarity (Figs 6D, 8C, D) and high correlation between N_0 estimated by the two methods[61] confirmed the adequacy of the visual selection. Statistical significance of N_0 changes was assessed applying the Chi-square test.

Computer simulations

A computational model was built using the programming language Object Pascal 9.0 in a Borland Delphi environment. The environment was arranged in such a way that it allowed construction of different models from standard pre-programmed modules.[40] The basic module represented a chemical synapse (Fig. 1A, B) with pre- and postsynaptic parts (1 and 2, respectively). The postsynaptic current (Fig. 1A, I_s) was calculated from the scheme shown in Fig. 1B, where R_s represents the subsynaptic resistance modified by the activation of receptor channels. The amount of transmitter released per presynaptic volley and therefore subsynaptic conductance ($1/R_s$) were assumed to depend on the presynaptic potential (V_p). We used a synaptic transfer (input–output) characteristic (Fig. 1C, continuous curve),[9,40] which reflects an increase in $1/R_s$ following presynaptic depolarization. It represents a modification of known dependencies[30,31,37] of the postsynaptic response amplitude on the presynaptic spike-like depolarization, specifically in the squid giant synapse.[31,37] The exact numerical characteristics of the synaptic transfer function (steepness and threshold) were variable even in the same preparation[31,37] and they are not known for the

hippocampal synapses. We used smaller steepness of the transfer function as compared to those published for the squid giant synapse[31,37] to account for possible partial inactivation of related voltage-dependent Ca^{2+} channels (VDCCs) and for changes in presynaptic spike amplitude in the presence of steady depolarization (see below). We also decreased the threshold of this dependence to account for the known data from experiments with steady KCl depolarization.[49] The data suggest that even a relatively small (about 20 mV) presynaptic depolarization is sufficient for a strong increase in the Ca^{2+}-dependent release. Approximately the same curve can be used to describe the release probability provided that it is $<<1$ at low V_p. In the simulations, we assumed $1/R_s = 0.3$ nS at $V_p = -70$ mV, which corresponds to the release of a single quantum in the MF synapse.[27] However, we simplified the analysis by not considering the stochastic quantal release. Nevertheless, it should be kept in mind that the positive feedback described by the model can occur only in synapses either having several release sites or able to produce multiple quantal release from a single release site (see Discussion). An important element of the electrical scheme of the chemical synapse is the synaptic cleft (gap) resistance (R_g; Fig. 1B). We considered R_g to be generally different from 0, unlike other extracellular resistances (R_{e1} and R_{e2} in Fig. 1A) ignored in Fig. 1B. Under voltage-clamp conditions, the presynaptic potential V_p (between points 1 and 3, Fig. 1B) deviates from the resting potential of the presynaptic membrane V_1 (between points 1 and 4, Fig. 1B) due to the potential drop V_g across R_g created by the postsynaptic current I_s:

$$V_p = V_1 - V_g. \tag{1}$$

Under the natural assumption $R_p >> R_g$, $V_g = I_s \cdot R_g$. Therefore,

$$V_p = V_1 - I_s \cdot R_g \tag{2}$$

and, according to the scheme (Fig. 1B),

$$I_s = V/(R_s \cdot (1 + R_g/R_s)), \tag{3}$$

where V is the postsynaptic potential between points 2 and 4 in Fig. 1B. The calculations of I_s from Eq. (3) are not trivial because of the positive ephaptic feedback mediated by the potential drop over R_g. As explained in the Results, the presynaptic potential V_p, which influences R_s (Fig. 1C), in turn depends on I_s. Therefore, iterations were used for the calculations.

In the case of paired stimulation with small (up to tens of milliseconds) intervals between the stimuli, the response (I_s) to the second pulse (EPSC2) is often larger than to the first (EPSC1) due to increased transmitter release, a phenomenon[68] known as PPF. To imitate the PPF at a 50-ms interval between two presynaptic volleys, the dependence $1/R_s$ from V_p for EPSC2 (Fig. 1C, dashed curve) was obtained by shifting to the left the basic EPSC1 curve.

RESULTS

Theoretical considerations of the positive ephaptic feedback in large chemical synapses

Before quantitative considerations, we shall describe the feedback qualitatively. The arrow I_s in Fig. 1A represents the EPSC generated by opening subsynaptic receptor channels (black box). The current produces a potential drop across the synaptic cleft resistance R_g (Fig. 1A, + and − in circles). The potential (point 3), which is negative relative to the extracellular space (point 4), would be applied to the presynaptic release site and would depolarize it. This fast depolarization would be added to the presynaptic depolarization induced by the presynaptic spike and would therefore increase transmitter release, thus creating a positive intrasynaptic feedback.[9,40]

This effect represents an example of non-chemical interneuronal interactions (see Refs 18 and 26 for reviews). Consistent with the definition of Jefferys,[26] we shall call this particular type of non-chemical interaction "ephaptic" to distinguish it from electrical coupling through gap junctions.[26 44] In some respects, the mechanism of this effect is analogous to the known ephaptic interaction in teleost medulla,[18] but the effect is of opposite sign. The strength of the positive intrasynaptic ephaptic feedback depends on the R_g value, similarly to the interaction between the Mauthner cell and neighbouring axons, which depends on a high resistance of the axon cap.[18,26]

The negative potential V_g (Fig. 1B) produced by the EPSC across R_g would depolarize the presynaptic release site. When V_g is large enough, it can result in an additional Ca^{2+} entry through VDCCs (Fig. 1A, thick arrow), leading to an enhancement of transmitter release. This positive feedback can be negligible in "typical" small central synapses with low R_g, but can be powerful in large synapses[9] with high R_g. We assumed that the feedback should be essential at MF–CA3 connections, where invaginations of pre- and postsynaptic membranes[11,45] lengthen the synaptic cleft and therefore increase R_g.

Another explanation of the feedback is illustrated by the dashed arrow (Fig. 1A), showing that a part of I_s would deviate at point 4 and flow through the presynapse. Here, it would produce a depolarization of the release zone (Fig. 1A, + and − over R_p), where the density of Ca^{2+} channels is maximum, thus increasing transmitter release. Both considerations are physically equivalent, but the second is more traditional,[55] whereas the first has the advantage of allowing a quantitative evaluation of the strength of the feedback on the basis of R_g values.

Our calculations are based on the presynaptic input–output function (Fig. 1C) similar to those obtained in experiments with application of presynaptic spike-like depolarization.[30,31,37] Therefore, this curve is valid for explanation of the feedback effect on the basis of fast additional depolarization induced by the EPSC itself. However, we used postsynaptic hyperpolarization to increase the EPSC amplitude. This may induce a steady presynaptic depolarization in synapses with large R_g (see below), with reduction in presynaptic spike height and transmitter release. This effect is the basis of the classical primary afferent depolarization explanation of presynaptic inhibition.[47] However, when the positive feedback is strong enough, any decrease in presynaptic spike amplitude can be overcome by increased transmitter release due to additional fast depolarization resulting from the increase in the EPSC amplitude under conditions of postsynaptic hyperpolarization. Moreover, the current branch illustrated by the dashed arrow (Fig. 1A; also see Fig. 2A) could even hyperpolarize a part of the presynapse, thus actually increasing spike amplitude. According to this scheme, the steady-state presynaptic depolarization occurs at the site of transmitter release, so that it should actually facilitate release processes.[43]

As noted above, in the presence of the positive ephaptic feedback, an intrasomatic hyperpolarization would increase EPSC amplitude more than expected from the shift in the driving force. The right part of Fig. 2A (Synapse 2) also shows that both branches of the hyperpolarizing current I_e (continuous and dashed curves) have the same direction as the EPSC of the same synapse. Therefore, similarly to the EPSC (Fig. 2A, I_{s2}), I_e should hyperpolarize a part of the presynapse (dashed arrow) and induce a depolarization at the release site (+ and − in circles over R_{g2}). Therefore, in addition to the above fast mechanism mediated by the positive feedback, the steady postsynaptic depolarization can induce a steady increase in transmitter release probability and a decrease in N_0, especially if the current does not induce a complete inactivation of presynaptic VDCCs (see Ref. 43

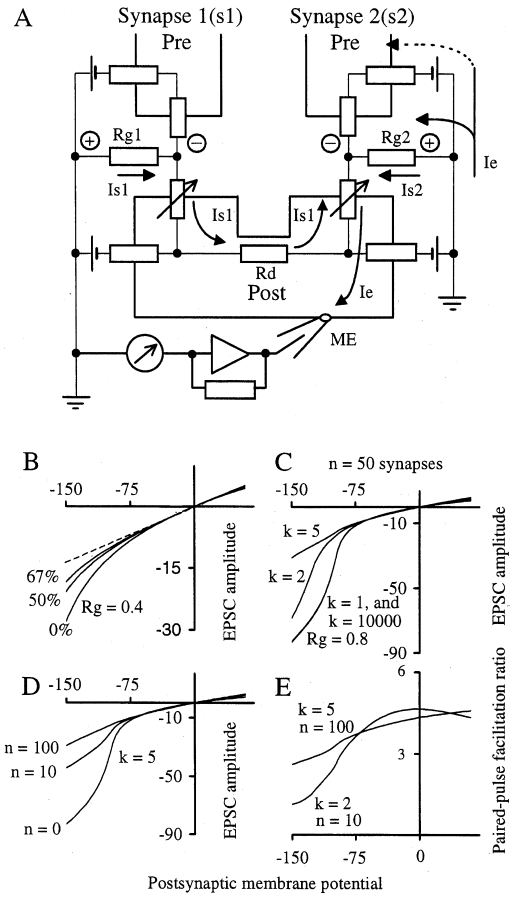

Fig. 2. Effects of activation of adjacent synapses in simulation experiments. (A) Scheme to show the current flow from activated Synapse 1 (I_{s1}) across the synaptic cleft resistance (R_{g2}) of the adjacent Synapse 2. Note that I_{s1} counteracts the action of both the hyperpolarizing current I_e applied through the intrasomatic microelectrode (ME) and the EPSC of Synapse 2 (I_{s2}). Both I_e and I_{s2} depolarize the presynaptic membrane in the vicinity of the release site of Synapse 2 (− and + in circles over R_{g2}). Note also that the I_e branch (dashed arrow) hyperpolarizes a part of the presynapse. See Fig. 1 for similar branch of I_s and for other notations. (B) A–V relationships for EPSCs generated by various proportions of synapses with linear A–V relationships added to a synapse with a non-linear A–V relationship and $R_g = 0.4$ GΩ. The proportion of the adjacent synapses is given in percentages at respective curves. The dashed line represents a linear A–V relationship ($R_g = 0$ for all synapses). (C–E) A–V relationships (C, D) and the PPF ratios (E) for various coefficients of attenuation of the signal along the dendrites (k) and various number of synapses with positive ephaptic feedback (n). The EPSC amplitudes in B–D were normalized to the mean amplitude obtained for a single synapse. Note that the increase in the percentage of synapses with linear A–V relations (B) and addition of synapses with attenuated signals (C, D) tend to linearize the A–V curves and to diminish the voltage dependence of the PPF ratio (E).

for additional effects of presynaptic depolarization). In contrast, EPSCs generated by neighbouring synapses would have an opposite action. Indeed, the current produced by synapse 1 (arrow I_{s1}) would produce a voltage drop across R_{g2} of a sign opposite to that produced by I_{s2} and I_e (Fig. 2A). Therefore, activation of adjacent synapses would diminish the positive feedback and counteract the facilitatory effect of the artificial postsynaptic hyperpolarization. As a result, the effects of postsynaptic hyperpolarization on large (composite) responses induced by activation of a large number of synapses can be smaller than its effect on minimal EPSCs. It should be mentioned that with EPSC recordings under conditions of perfect voltage clamp, no current is flowing between adjacent synapses, but this condition is difficult to achieve in practice, when not only synapses proximal to the cell body but also remote synapses are activated.

Computer simulations

Ephaptic feedback. To evaluate the influence of the ephaptic feedback in a more quantitative way, the dependence of the EPSC amplitude (I_s in Fig. 1A) on R_g was calculated. Assuming $R_p >> R_g$, the presynaptic part of Fig. 1B can be ignored. According to the Ohm law under clamped potential, the postsynaptic potential between points 2 and 4 (Fig. 1B) is given by:

$$V = I_s \cdot (R_g + R_s), \tag{4}$$

where the subsynaptic membrane conductance $1/R_s$ is an increasing function of the presynaptic potential V_p (Fig. 1C). Due to the presence of the intrasynaptic feedback, V_p is also a function of I_s [see Eq. (2)]. We calculated I_s from the system of Eqs. (2) and (4) using iterations. In order to study the effect of the ephaptic feedback on I_s (i.e. on the EPSC amplitude), R_g was varied (Fig. 1D). As considered in the Discussion, R_g in the MF synapses could be as large as hundreds of megaohms. A large (supralinear) increase in the EPSC amplitude at negative MPs in the presence of the feedback ($R_g > 0$) is shown in Fig. 1D. For instance, at −100 mV and $R_g = 0.4$ GΩ, the amplitude was about 50% larger than that in the absence of the feedback ($R_g = 0$). The supralinearity increased with increasing R_g values (Fig. 1D). These numerical dependencies have been obtained with the transfer function (input–output curve) shown in Fig. 1C. The strength of the feedback depends not only on R_g, but also on the threshold and steepness of the input–output curve. As explained in the Experimental Procedures, we suggested that the steepness is generally smaller than that obtained in the squid synapses.[31,37] With larger steepness, hyperpolarization effects would be stronger even at smaller R_g values. Because of the lack of exact parameters of synaptic transmission, our model considerations should be regarded as semi-quantitative rather than strictly quantitative. Nevertheless, the validity of the estimated dependencies is supported by physiological data (see below).

Effects of the ephaptic feedback on amplitude–voltage relations. In Fig. 1D it is seen that while, at $R_g = 0$, the A–V relation was linear, this became "supralinear" at negative potentials when the ephaptic feedback was present ($R_g > 0$). Note also that the relation was "underlinear" at positive MPs (Fig. 1D). This effect is due to the EPSC reversal that converts positive intrasynaptic feedback into negative because of the opposite sign of the potential drop across R_g.

Voltage dependence of paired-pulse facilitation in synapses with ephaptic feedback. When two EPSCs (EPSC1 and EPSC2) were evoked with a sufficiently short interval (e.g. 50 ms), PPF was found at many synapses,[68] including hippocampal ones (for review, see Ref. 58). Changes in the PPF ratio provide an index of variations in presynaptic release probability.[68] We evaluated the influence of several variables (V_p, R_g and V) on PPF using the dependencies shown in Fig. 1C for EPSC1 and EPSC2 (continuous and dashed lines, respectively). The results of computer experiments using different R_g values are illustrated in Fig. 1E. Because of its purely presynaptic nature,[58,68] PPF was voltage independent

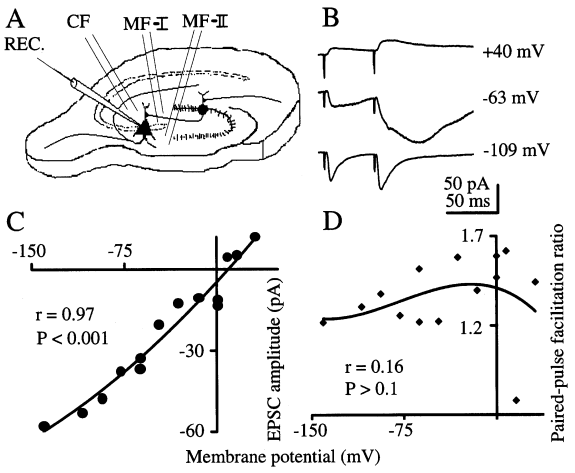

Fig. 3. Effects of different holding potentials on composite EPSCs in physiological experiments. (A) Arrangement of recording (REC) and stimulating electrodes positioned to activate the CFs and the MFs (MF-I and MF-II). (B) Superposition of averages ($n = 20$) at indicated holding potentials. (C) $A–V$ relationship for the same experiment. (D) Plot of the PPF ratio against MP. The curves in C and D represent third-order polynomial fits of the experimental points. Coefficients of the linear regression (r) with their significance levels (P) are also given. The high r in C signifies that the dependence does not differ significantly from linear theoretical prediction. The low r in D indicates that PPF is voltage independent.

in the absence of the feedback ($R_g = 0$), but showed complicated voltage dependencies at $R_g > 0$.

Effects of activation of multiple inputs. To simulate activation of adjacent synapses, the respective equations were solved for two equivalent electrical schemes similar to Fig. 1B and connected with a resistance R_d (Fig. 2A). The latter imitated dendritic attenuation of the signal and varied from 0 (no attenuation, i.e. attenuation coefficient $k = 1$) to infinity (complete electrical separation of remote synapses). In practice, to imitate the separation we used k equal to several thousand (10,000 in Fig. 2C). First, we studied the influence of activation of additional electrotonically close synapses ($R_d = 0$) without feedback (Fig. 2B). As expected, $A–V$ relation linearity improved with increased proportion of synapses without feedback (Fig. 2B). Next, we tested possible feedback reduction, when adjacent synapses even with ephaptic feedback were activated under conditions of imperfect voltage clamp. Signal attenuation (k) and the number of adjacent activated synapses (n) were varied. Cases with a fixed number of adjacent synapses ($n = 50$) and attenuation absent ($k = 1$) or very large ($k = 10{,}000$) are illustrated in Fig. 2C (lower curve). In both cases, the $A–V$ relation was about the same and indistinguishable from that of a single synapse with the same ephaptic feedback. In contrast, the $A–V$ curve became almost linear at $k = 5$ (Fig. 2C). Simulations in which n was varied while k was maintained constant are illustrated in Fig. 2D. The increase in the number of synapses not perfectly clamped made the $A–V$ relation more linear in spite of the large R_g (0.8 GΩ) in each synapse (Fig. 2D, compare $n = 0$ and 100).

Effect of multiple inputs on paired-pulse facilitation. Making the $A–V$ relation more linear, addition of neighbouring synapses should influence PPF voltage dependence. This suggestion was confirmed in simulations in which both k and n were varied. In Fig. 2E, it is seen that for the coefficient of attenuation $k = 2$, the PPF voltage dependence for 10 activated synapses was not strongly different from that for one synapse ($R_g = 0.8$; Fig. 1E). For $k = 5$ and a larger number of synapses ($n = 100$; Fig. 2E), the dependence was smaller: the PPF ratio increased <40% when the MP was changed from −100 to 0 mV.

Physiological experiments

The computer modelling predicted presynaptic effects of postsynaptic hyperpolarization and also different $A–V$ dependencies for large and small synaptic currents. We tested these predictions in electrophysiological experiments. These are described below under subheadings specifying five key predictions.

Amplitude–voltage dependence of composite excitatory postsynaptic currents is close to linear. Averages ($n = 20$) of composite EPSCs evoked by MF stimulation (MF-I, Fig. 3A) at three different holding potentials in a single neuron are shown in Fig. 3B. The absence of response failures confirmed that a large number of presynaptic fibres were activated. The EPSC amplitude increased during hyperpolarization and reversed its sign at positive MPs (Fig. 3B, C). The $A–V$ relation was linear: the polynomial fitting of the experimental points appeared to be very close to a straight line and the coefficient of the linear correlation was highly significant (Fig. 3C, $r = 0.97$). Similar linear $A–V$ relations were found in seven of 10 experiments in which EPSCs were evoked by MF stimulation (MF-I or MF-II, Fig. 3A). In three of 10 cells, the $A–V$ curve rectified in the outward direction at hyperpolarized MPs (Fig. 4B). As a result, the average curve for all 10 neurons (Fig. 5A) showed a small "underlinearity" at negative MPs, but the deviation from the linear prediction (dashed line) did not reach the significance level ($P = 0.07$ at −109 mV). Similar linear $A–V$ relations were observed for composite EPSCs evoked by CF stimulation (CF in Fig. 3A, $n = 4$ cells, Fig. 5B).

Paired-pulse facilitation of composite excitatory postsynaptic currents is voltage independent. We applied paired pulses with 50-ms inter-pulse intervals (Fig. 3B) and calculated PPF ratios at various MPs (Fig. 3D). In spite of some variability, especially at MPs around 0, where the responses were relatively small, the PPF ratio was voltage independent, as shown by the polynomial fit close to linear (with a slope not significantly different from 0, $r = 0.16$, $P > 0.1$; Fig. 3D). Altogether PPF ratios at 50-ms inter-pulse intervals were calculated at different MPs for eight MF EPSCs. Six neurons showed PPF. The PPF ratios varied from 1.37 to 5.31 (2.94 ± 0.80, mean ± S.E.M.). In four of six neurons, no significant voltage dependence was found (Fig. 3D). Two neurons showed PPF voltage dependencies qualitatively similar to those predicted from the model with the ephaptic feedback (Fig. 1E, $R_g > 0$). An example (Fig. 4C) shows clear voltage dependence. However, the overall linear fit had a slope not different from 0 ($r = 0.04$). The mean data from all six cells showed only a trend to voltage dependence (Fig. 5C). Neither the linear regression nor the differences between the PPF ratio at hyperpolarized and 0 mV MPs were statistically significant ($P > 0.1$).

Postsynaptic hyperpolarization induces supralinear

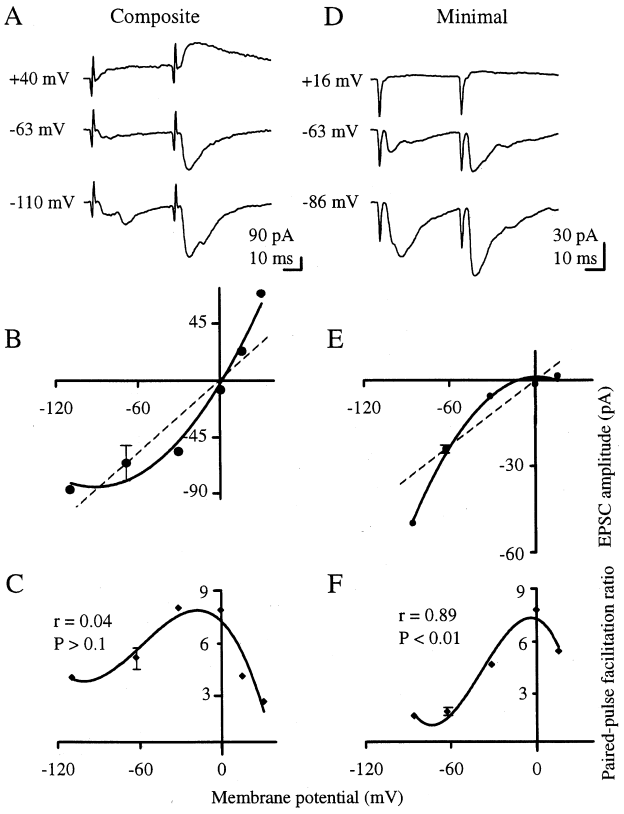

Fig. 4. Comparison of the voltage dependencies of composite (A–C) and minimal (D–F) EPSCs evoked in the same neuron by strong and minimal MF stimulation, respectively, at the indicated membrane potentials. (A, D) Examples of averaged EPSCs at different MPs. (B, E) $A–V$ plots. Dashed lines represent linear predictions crossing the amplitude at −63 mV and the point with 0,0 coordinates. (C, F) Plots of the PPF ratios vs holding potentials. All measurements were obtained from averaged waveforms. For the "resting" holding potential (−63 mV), the measurements were repeated ($n=4$) and the means are given together with ±S.E.M. See Fig. 3 for other explanations.

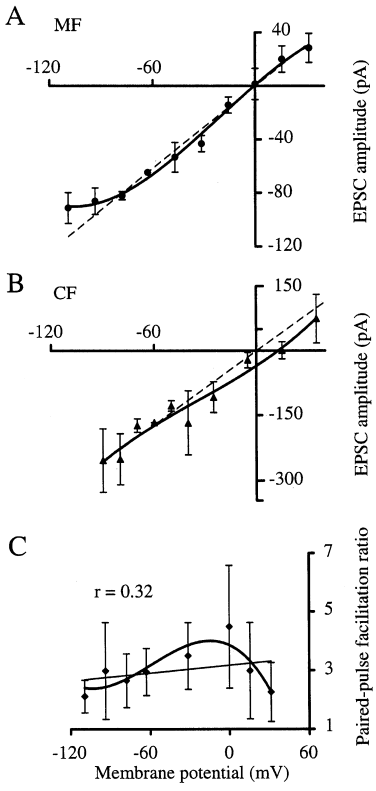

Fig. 5. Summary of $A–V$ relationships (A, B) and voltage dependencies of the PPF ratio (C) for composite EPSCs. (A, B) Data for EPSCs elicited with MF (A; $n=10$) and CF stimulation (B; $n=4$ neurons; means ± S.E.M.). EPSC amplitudes at different MPs were divided by the value at −63 mV and were multiplied again by the mean current value at −63 mV from different experiments. (C) Data for MF EPSCs ($n=6$). The thin line in C represents the linear regression ($r=0.32$ is not significantly different from 0, $P>0.1$). See Fig. 3 for other notations.

amplitude increase and reduces failure rate of minimal excitatory postsynaptic currents mediated by large synapses. The hypothesis and modelling predict supralinear increase in the amplitude of single fibre EPSCs distinct from the above linear $A–V$ relations for composite EPSCs. To test this difference, composite and minimal EPSCs were compared at "resting" and at hyperpolarized MPs. In Fig. 6A, the amplitudes of minimal MF EPSCs evoked at −63 and −93 mV are plotted against time. With hyperpolarization, the increase of EPSC amplitude was more than expected from the −30 mV MP shift (see Fig. 7D) and it was accompanied by a reduction in N_0. We calculated N_0 by separating failures visually (Fig. 6B, C) or by doubling the number of positive responses. According to both methods, N_0 decreased during hyperpolarization (Fig. 6D, empty and striped columns). Similar N_0 reduction was seen in the amplitude distributions (Fig. 6E), where the dashed columns represent background noise. The modification of the shape of the distribution due to hyperpolarization (Fig. 6E, −93 mV) cannot be explained by a linear re-scaling of the control distribution (Fig. 6E, −63 mV), as would be expected from the classical $A–V$ relation. Composite EPSCs recorded from the same neuron following a stronger MF stimulation, so that failures disappeared and amplitude fluctuations were strongly reduced, are shown in Fig. 7A. At −93 mV, the amplitude increased, but the increase was significantly smaller than for minimal EPSCs (Fig. 7C, D). The latter showed clear "supralinear" increase during hyperpolarization (Fig. 7D, small symbol). The same statistically significant difference was evident in the summary data for all six minimal and composite MF EPSCs recorded from the same neurons (Fig. 7E, $P<0.01$, t-test for matched pairs).

The MF synapses are typically much larger than the CF synapses and therefore should posses larger R_g and should exhibit larger hyperpolarization effects. The effects of the MP shift on minimal EPSCs induced by MF and CF stimulation in the same neuron are compared in Fig. 8. Although both inputs showed significant changes in N_0 (Fig. 8C–F), the increase in the amplitude of the MF EPSC was larger (Fig. 9A). The experimental points for minimal CF EPSC amplitudes (Fig. 9A, small triangles) were close to the linear prediction and to the $A–V$ relations for composite EPSCs recorded from the same neuron (Fig. 9A, large symbols). The mean relative amplitude of minimal CF EPSCs recorded at −93 mV in three other experiments was also close to the linear prediction (129 ± 5%). In contrast, the location of the experimental point for the minimal MF EPSCs indicates strong supralinear voltage dependence (Fig. 9A, small filled circle at −80 mV). Altogether, statistically significant ($P<0.03$, at least) supralinear amplitude increase and N_0 reduction were observed in five of seven minimal MF EPSCs (see summary plots of Fig. 9B and C). Different hyperpolarization effects in two inputs to the same neurons suggest

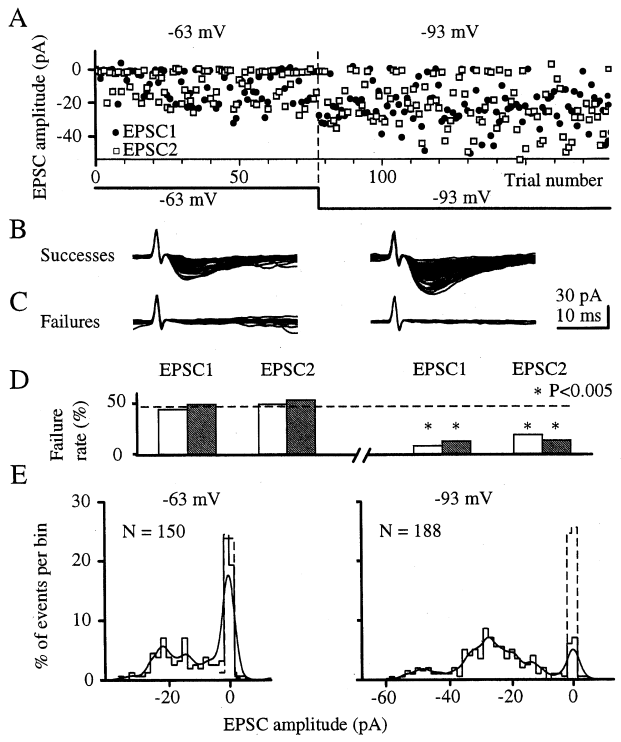

Fig. 6. Effects of postsynaptic hyperpolarization on minimal EPSCs. (A) Plot of amplitudes of minimal EPSCs induced by the first (EPSC1, dots) and second pulses (EPSC2, squares) in the paired-pulse paradigm. (B, C) All EPSC1 successes (B) separated visually from failures (C). (D) Failure rates determined by visually selecting failures and doubling the number of positive amplitudes (open and hatched columns, respectively). Asterisks mark significant differences as compared to −63 mV (Chi-square test). The dashed line marks the mean control failure rate for EPSC1, which was very close to that for EPSC2 in this experiment. (E) Amplitude distributions from the same experiment. Conventional and smoothed distributions are given. The dashed columns represent noise distributions. Amplitudes of EPSC1 and EPSC2 were pooled. Note a large difference between the first peaks in the two distributions, which contain response failures (amplitudes similar to the noise values).

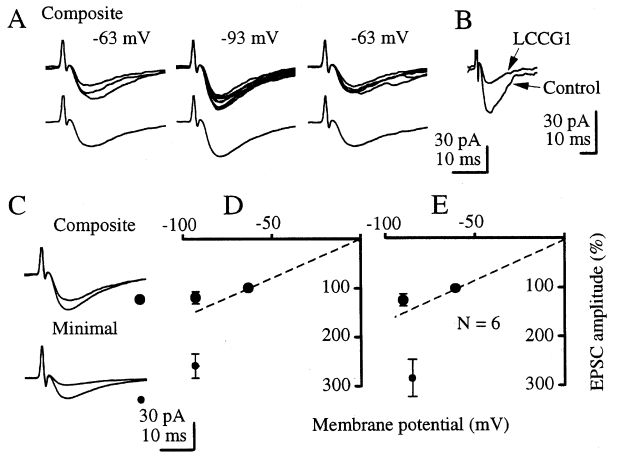

Fig. 7. Comparison of effects of postsynaptic hyperpolarization on composite and minimal EPSCs recorded from the same neurons. (A) Single (upper raw) and average (lower raw) EPSCs evoked in the same neuron as in Fig. 6 after increasing stimulus strength (×1.3). (B) Superposition of the averaged EPSCs induced before (lower trace) and during 10 μM L-CCG-I bath application (upper trace). The depressing L-CCG-I effect suggests activation of MFs. (C) Superpositions of averaged composite (upper raw) and minimal EPSCs (lower raw) at −63 and −93 mV to show a stronger hyperpolarization effect on the minimal EPSCs. Amplitude calibration for composite EPSCs is the same as in A. (D) Amplitudes of the composite and minimal EPSCs from the same experiment (larger and smaller symbols, respectively) plotted against two MPs (resting and hyperpolarized). The amplitude at −63 mV is taken as 100%. (E) Similar summary plot for six minimal EPSCs (small filled circle) recorded from the same neurons as composite EPSCs (large filled circles). The dashed lines in D and E show linear predictions with the equilibrium potential at 0. Note that the experimental points for composite EPSCs are close to the linear prediction, while in the same neurones, the amplitudes of minimal EPSCs significantly deviated from the classical prediction at −93 mV, showing strong "supralinearity" ($P < 0.01$). Means ± S.E.M. are shown in D and E at the hyperpolarized holding potential.

that the deviation from linearity in the MF input was not due to general alterations in the postsynaptic neuron or changes in the recording conditions.

The amplitude–voltage relation for minimal excitatory postsynaptic currents is non-linear. In the above experiments, minimal EPSCs were compared only at two different MPs (Figs 6–9). For 12 minimal MF EPSCs, we obtained stable data for the $A-V$ curves (see Experimental Procedures for the control of stability). In four of 12 inputs, the curves for both composite and minimal EPSCs were constructed from the same neurons. In the example of Fig. 4A and B, composite EPSCs showed "underlinear" $A-V$ dependence at hyperpolarized MPs. In contrast, minimal EPSCs showed "supralinear" increase at hyperpolarized potentials (Fig. 4D, E) similar to that in simulations of the ephaptic feedback (e.g. Fig. 1D, $R_g = 0.4$). Altogether, the $A-V$ curves for nine of 12 minimal EPSCs showed "supralinear" dependencies so that the summary curve (Fig. 10A) showed a statistically significant ($P < 0.05$) difference between the linear prediction (dashed line) and the experimental points at −109 mV. In addition, at positive potentials (Fig. 10A), "underlinear" deviation from the linear dependence was observed ($P < 0.05$) in accordance with respective results of simulation experiments (Fig. 1D).

Paired-pulse facilitation of minimal excitatory postsynaptic currents is voltage dependent. PPF ratios for composite and minimal EPSCs recorded from the same neuron are compared in Fig. 4C and F. In comparison with the composite EPSC, the increase in PPF of the minimal EPSC during depolarization from −63 to 0 mV was larger (about 1.5 and 5.5 times, respectively). The polynomial fit for the minimal EPSC resembled the dependence predicted from the model with the ephaptic feedback (Fig. 1E, $R_g = 1.6$). Altogether, paired-pulse experiments were performed on eight neurons. At 50-ms inter-pulse interval, six MF EPSCs showed PPF with ratios ranging, at −63 mV, from 1.34 to 5.46 (mean 3.03 ± 0.80). In four of six cells, the PPF ratio increased during depolarization, as exemplified in Fig. 4F. As expected for R_g variations across synapses (Fig. 1E), the voltage dependencies varied quantitatively in different neurons. In spite of this variability, the summary data (Fig. 10C) showed that PPF at −109 mV was significantly smaller than that at −63 mV ($P < 0.05$, t-test for matched pairs, $n = 6$).

DISCUSSION

The present work was designed, firstly, to test Byzov's hypothesis on intrasynaptic ephaptic feedback[8,40,60] using EPSCs mediated by large MF synapses which are particularly suitable for such analysis and, secondly, to resolve contradictions on hyperpolarization effects. In contrast with numerous published linear $A-V$ relations,[3,21,27] previous findings of

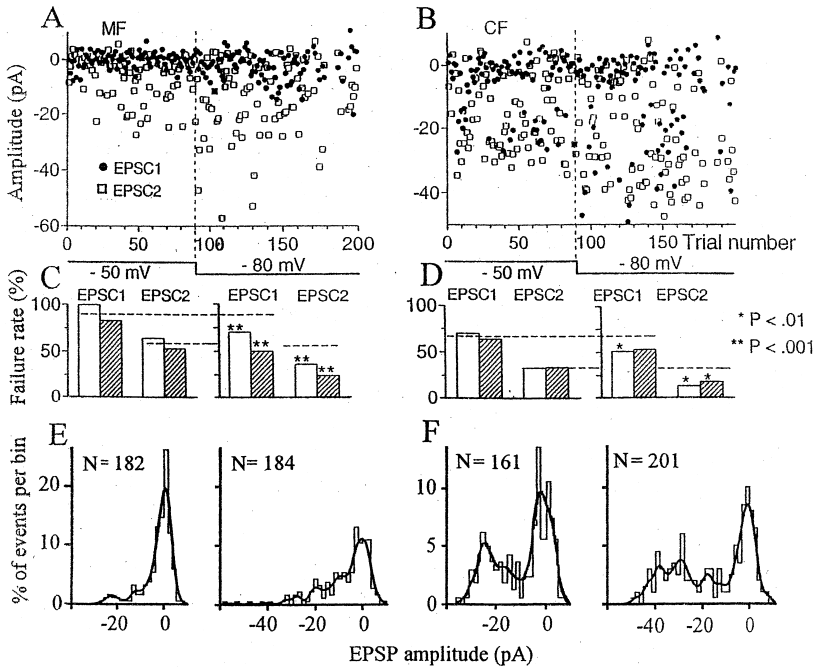

Fig. 8. Effects of postsynaptic hyperpolarization on minimal EPSCs evoked by MF and CF activation. (A, B) Amplitudes of minimal EPSCs evoked in the same neuron by MF (A) or CF stimulation (B) at two holding potentials. (C, D) Failure rates determined for EPSC1 and EPSC2 as in Fig. 6D. (E, F) Amplitude distributions as in Fig. 6E. Note that failure rates decreased during hyperpolarization in both inputs in this experiment, but the decrease was statistically more significant in the MF (C) as compared to the CF input (D). Note also stronger changes in the distributions of MF EPSC amplitude (E) as compared to those for the CF EPSC (F).

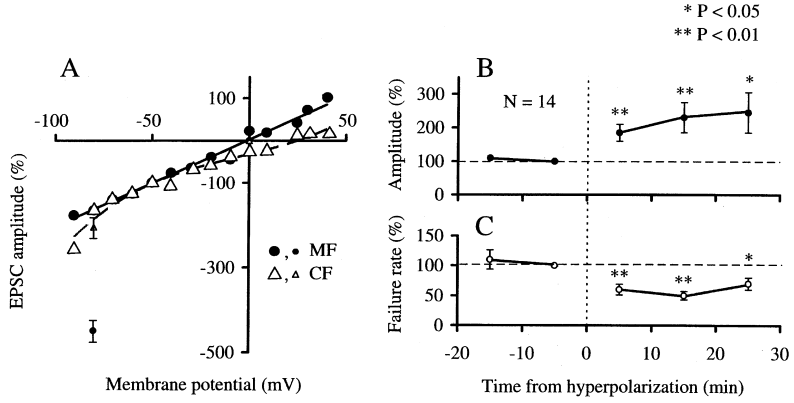

Fig. 9. Summary data of the effects of postsynaptic hyperpolarization on minimal EPSCs. (A) Comparison of $A-V$ plots for composite EPSCs (larger symbols) with amplitudes of the minimal EPSCs at two MPs (−50 and −80 mV, smaller symbols). Data from the same neuron shown in Fig. 8. Dots and triangles, data for the MF and CF EPSCs, respectively. Continuous (MF) and dashed lines (CF) represent polynomial fits for the composite EPSCs, which are very close to linear fits. Note that the experimental data for the minimal CF EPSC (see the small triangle at −80 mV) are close to the fit for the composite EPSCs, while similar points for the minimal MF EPSC (see the small filled circle at −80 mV) indicate a strong deviation from the linear dependence during hyperpolarization. (B, C) Summary of amplitude (B) and failure rate changes (C) obtained from seven minimal MF EPSCs. The data for EPSC1 and EPSC2 were pooled. Data over consecutive 30 trials (about 8 min) were normalized to the 30 trials obtained immediately before hyperpolarization. Statistical significance of the differences from the controls was assessed by the *t*-test for matched pairs.

changes in indices of transmitter release during postsynaptic hyperpolarization[61] suggested non-linear $A-V$ relations. To resolve this contradiction, we performed computer simulations and compared physiological recordings of minimal and composite MF EPSCs. The simulations gave several predictions, which were confirmed experimentally. This resolves the above contradiction related to voltage dependencies of hippocampal EPSCs. In general, our data strengthen the intrasynaptic feedback hypothesis. Independently of this interpretation, we presented a number of novel findings suggesting the existence of novel mechanisms whereby postsynaptic MP changes control presynaptic release.

Comparison of minimal and composite excitatory postsynaptic currents

Our results are in agreement with literature data showing linear $A-V$ relations[3 21,27] and the lack of voltage dependencies of indices of presynaptic release[12,38] calculated from recordings of composite EPSCs. The $A-V$ relations for minimal EPSCs have not been studied in detail so far. Nevertheless, a published example[46] shows a supralinear amplitude increase of a CA1 EPSC during hyperpolarization. No nonlinear differences between amplitude distributions of five minimal CA1 EPSCs recorded at two MPs have been reported

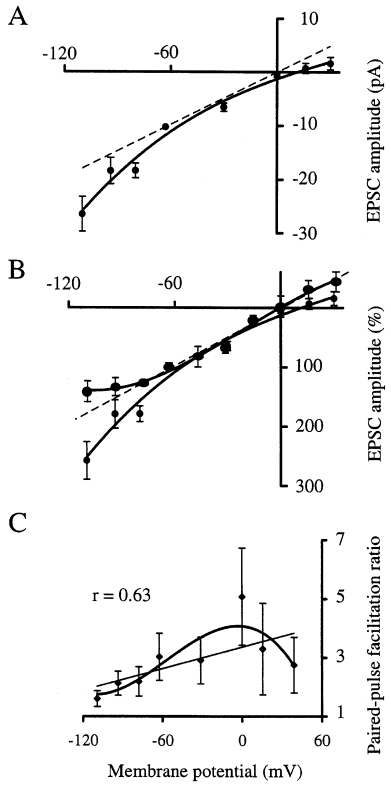

Fig. 10. Summary of $A-V$ relationships (A, B) and PPF voltage dependence (C) for minimal EPSCs. (A) Data for 12 minimal MF EPSCs. (B) Repetition of A given as percentages relative to the "resting" holding potentials with superposition of the $A-V$ plot for composite EPSCs (larger symbols, data from Fig. 5A). Note that deviations from the linear prediction (dashed line) are different for the polynomial fits of data related to the composite and minimal EPSCs. (C) Data from six neurons. Note that the coefficient of linear regression ($r = 0.63$), although not significant for this small sample, was larger than that for the composite MF EPSCs in Fig. 5C. See Fig. 5 for other explanations.

by Kullmann and Nicoll.[34] However, in the CA1 region, supralinear hyperpolarization effects are rather rare,[61] and in the published example (Fig. 2)[34] response failures were absent. It has also been reported[17] that postsynaptic hyperpolarization affects only quantal size of minimal depolarizing inhibitory postsynaptic currents in one dentate gyrus neuron, suggesting a linear $A-V$ relation. However, in spite of the fact that failures were excluded from the published distribution (Fig. 8),[17] changes in separate peaks are difficult to explain only by driving force shifts. We conclude that our data have no clear disagreement with known literature and that they reveal novel properties of minimal (single fibre) responses.

Ephaptic feedback in mossy fibre–CA3 synapses

In addition to supralinear amplitude increases during hyperpolarization, our simulations predicted that, when the feedback is sufficiently strong, the $A-V$ curve at positive potentials becomes "underlinear". The reason is that the EPSC reverses its sign at positive MPs and therefore would generate negative rather than positive feedback. Our physiological data confirmed both the supralinear amplitude increase during postsynaptic hyperpolarization and "underlinear" dependency at positive MPs.

The strength of the feedback is determined by several factors, especially by R_g, which are likely to be specific for each synapse because of their variable morphology (see below). Therefore, results are expected to vary widely from one experiment to the next. Nevertheless, the summary $A-V$ curve (Fig. 10A) shows significant deviations from linearity, suggesting large average efficacy of the ephaptic feedback in the MF–CA3 synapses.

A theoretical evaluation of the feedback efficacy has been done for a retinal chemical synapse.[9] The key value is the potential drop V_g across R_g. From Fig. 1B, $V_g = V_{24} \cdot R_g/(R_g + R_s)$, where V_{24} is the potential between points 2 and 4. Therefore, the ratio $K = R_g/(R_g + R_s)$ can be called "the coefficient of intrasynaptic feedback". It has been evaluated[9] assuming a cleft width of 20 nm and $R_s = 1\ \Omega \cdot cm^2$ as for the activated neuromuscular junction.[29] For a small flat synapse of about 0.3 μm diameter, $K = 0.01$ and therefore the feedback would be negligible.[9] However, with a thin (0.1 μm) postsynaptic process invaginating 1 μm deep into the presynaptic membrane, $K = 0.5$, so that the additional presynaptic depolarization due to the ephaptic feedback reaches a considerable part of the excitatory postsynaptic potential (EPSP) amplitude. Electron microscopy data[11,45] have shown that, in the stratum lucidum of the CA3 area, "spinules", which are processes of dendritic spines, penetrate large (about 4 μm diameter) presynaptic boutons. Typical spines diameters are about 0.4 μm (0.2–1 μm).[45] Assuming a cleft width of 20 nm, it is possible to estimate the lower and upper bounds of R_g. For a "thin" spinule (0.2 μm in diameter) penetrated through the whole of the presynaptic bouton (4 μm), R_g would vary from 177 to 708 MΩ depending on the specific cleft resistivity[63] (from 50 to 200 Ω·cm). R_g would range from 84 to 335 MΩ for a spinule of 0.4 μm diameter and from 32 to 130 MΩ for a "thick" (1 μm) spinule. Assuming $R_s = 3$ GΩ, which corresponds to a single quantum release,[27] the above estimates suggest that, when spinules are thin, an essential part of the EPSC drops across the synaptic cleft ($K = 0.06$–0.24). These estimates give only rough approximations. Additional factors can influence R_g and R_s, and therefore K. These include a possible higher resistivity of the extracellular matrix in the synaptic cleft, and the presence of barriers ("corks") between the synaptic cleft and the extracellular space created by glial cells,[60] as well as multiquantal release. In these cases, the feedback would be effective even for thinner and shorter spinules.

Our simulations demonstrated that addition of synaptic inputs either with imperfect clamp or without intrasynaptic feedback would linearize the $A-V$ relation. This explains apparent contradictions between our previous results[61] and data reported in the literature.[3,27] Our physiological experiments directly demonstrated differences between minimal and composite EPSCs. In Fig. 10B, normalized $A-V$ relations for the composite and minimal EPSCs are superimposed and compared with the linear prediction (dashed line). At −109 mV, the mean amplitude of the minimal EPSCs was 1.5-fold larger than that expected from the linear $A-V$ relationship and 1.8-fold larger than that for the composite EPSCs. The mean $A-V$ curve for the minimal MF EPSCs is slightly more "supralinear" than that obtained in simulation experiments for $R_g = 0.5$ GΩ and $K = 0.2$. These values are in striking agreement with respective estimations made above for MF synapses with the thin spinules. These considerations suggest that, on average, at resting MP, the ephaptic feedback is moderate, although it should influence EPSC amplitude. Also, the strong average hyperpolarization effect

(−109 mV; Fig. 10A) indicates that MP shifts would effectively influence presynaptic release. Stronger than average non-linearity in some experiments (Fig. 4E) could suggest larger R_g and K (about 1 GΩ and 0.3, respectively), and effective influences of the feedback already at resting MP.

The differences between the hyperpolarization effects on synapses made by the MF and CF were noted here and investigated in more detail elsewhere.[6] This difference, together with smaller hyperpolarization effects on Schaffer collateral–CA1 responses,[61] can be considered as additional support to our hypothesis. This difference could be at least partially related to different distances from the soma and hence different clamp efficacies. However, clear difference was recently demonstrated also under conditions of current clamp recordings.[6] Simulation studies have shown that attenuation of the constant current along the dendrite is small.[53]

We noted above that we used the simplest scheme with a single release site and without considering EPSC time-courses to simplify the feedback illustration. It is clear that the proposed feedback acts after the release event has already taken place. Hence, it is only the subsequent releases that are affected by the feedback. Recent recordings from putative single synapses at CA1 demonstrated a strong suppression of EPSCs evoked at short intervals, suggesting a short-term synaptic depression after a prior exocytotic event.[15] This observation seems to be in contradiction to the intrasynaptic ephaptic feedback hypothesis that supposes additional transmitter release immediately after EPSC generation. More detailed considerations (Ref. 60 and unpublished simulations) show that the ephaptic feedback mechanism is readily applicable to synapses with multiple release sites similar to giant MF–CA3 synapses. Accordingly, for a junction with multiple release sites, no depression was found at short intervals following previous release.[64] Consistent with the hypothesis, notches on the rise of multiquantal MF EPSCs can be detected, revealing delays in releases of successive transmitter quanta (vesicles).[27]

Could membrane capacitance affect the ephaptic feedback?

For computer simulations, several simplifications were introduced and one is that we did not consider time-courses (only EPSC amplitudes) and therefore neglected capacitances. However, under voltage-clamp conditions, the influence of capacitors is negligible. Even under conditions of imperfect voltage clamp, capacitors cannot critically influence the feedback in the sense of abolishing it. Capacitors may diminish EPSC amplitude, thus reducing the feedback, but for our considerations the absolute EPSC amplitude is of secondary importance. In fact, if capacitances are considered, the ephaptically transmitted feedback signal (potential drop V_g in Fig. 1B) should be only slightly reduced in addition to its natural change due to the diminution of the EPSC amplitude. It is difficult to evaluate the exact value of the capacitance associated with the synaptic gap resistance (R_g), but it should be very small in comparison with the postsynaptic membrane capacitance. Therefore, the kinetics of the feedback depolarization should not be essentially slower than the kinetics of the EPSP generated in the dendritic spine and the EPSC amplitude should not significantly decrease.

Voltage dependence of paired-pulse facilitation

It was expected that, in synapses with ephaptic feedback, PPF would decrease with hyperpolarization and increase with depolarization due to respective changes in the probability of transmitter release. However, our simulations showed that, generally, the voltage dependence of PPF is more complicated (Fig. 1E). Thus, the PPF ratio was voltage independent for large membrane hyperpolarizations and large feedback. The explanation is that, under these conditions, transmitter release probability would be close to saturation (theoretically to 1) already for EPSC1, so that the second pulse cannot be more effective. At less hyperpolarized MPs, the PPF ratio would increase because of a decrease in release probability. A seemingly paradoxical asymmetry of the curve around 0 is explained by the interplay of two factors: classical EPSC voltage dependence, which strongly diminishes amplitudes of both EPSC1 and EPSC2 at small negative MPs, and subsequent changes in the sign of the feedback at positive potentials.

Possible complications due to steady presynaptic depolarization

Our model is based on the presynaptic input–output function (Fig. 1C), similar to that obtained in experiments with application of spike-like depolarization.[30,31,37] These experiments clearly showed that the larger the presynaptic depolarization, the larger the transmitter release. Therefore, the fast ephaptic feedback should increase transmitter release due to additional fast presynaptic depolarization. One complication is that, to test the presence of the positive feedback, we increased the EPSC amplitude using steady MP hyperpolarization. If this hyperpolarization induces appreciable steady depolarization shift presynaptically, it can inactivate presynaptic VDCCs and therefore change the input–output function. We used a smaller steepness as compared to the published functions,[31,37] to account for a partial VDCC inactivation. We believe that the inactivation should be incomplete on the bases of known strong Ca^{2+}-dependent transmitter release in central synapses during steady K^+ depolarization.[49] It is also known that presynaptic depolarization strongly increases spontaneous transmitter release[22,36] and can strongly facilitate evoked transmitter release.[43] As we have noted, quantitative changes in the synaptic transfer function should influence the effects of the feedback in the sense that the same R_g values would produce larger or smaller feedback effects. Therefore, for the present semi-quantitative description of the feedback, the exact numerical characteristics of the transfer function are not very important provided that its basic shape remains the same, i.e. transmitter release is an increasing function of the fast presynaptic depolarization.

Alternative hypotheses

We have previously discussed several alternative explanations and found them less likely than the ephaptic feedback hypothesis.[6,61] Theoretically, non-linear voltage dependencies could result from postsynaptic interactions between *N*-methyl-D-aspartate receptor-gated conductances, VDCCs and non-ideal voltage clamp. However, the involvement of *N*-methyl-D-aspartate receptors can be excluded, because strong non-linear effects have also been observed in the presence of *N*-methyl-D-aspartate receptor antagonists.[6,59] Among VDCCs, the most likely candidate is the low-threshold

T-type calcium channel,[23] whose inactivation could be reduced by membrane hyperpolarization. However, VDCCs have been shown to be activated only under current-clamp conditions, when composite EPSPs reach 15–20 mV amplitude,[39] and they contributed to the peak rather than to the initial slope of the EPSCs. Therefore, this mechanism could hardly explain the supralinear increases in small EPSCs recorded here, changes in indices of presynaptic transmitter release[6,59,61] and the lack of non-linear changes in large EPSCs.

Several theoretical possibilities could explain the presynaptic effects of postsynaptic hyperpolarization.[6,61] One possibility is changes in extracellular ionic concentration resulting in alterations of transmitter release. However, early data from the neuromuscular junction[55] suggest that the major effect of postsynaptic hyperpolarizing current is a reduced K^+ concentration around the synaptic terminal, associated with a reduction in transmitter release rather than with its increase. Concentration of the major extracellular cation, Na^+, could theoretically decrease with postsynaptic hyperpolarization. However, the changes should be negligible because its concentration is high outside, and the major expected effect would again be EPSC decrease. An increase in the concentration of the major extracellular anion Cl^- with hyperpolarization should also be negligible, especially taking into account its reversal potential (−70 mV). These changes cannot essentially influence EPSC amplitude, because glutamate-activated channels are not permeable to Cl^-. Accordingly, in experiments with depolarization to 0 mV, we did not see outward currents.

The most obvious alternative to the ephaptic feedback is that postsynaptic hyperpolarization suppresses release of a retrograde messenger, which at rest would inhibit presynaptic transmitter release. A possible candidate is glutamate.[20] Glutamate is known to inhibit presynaptic release acting on inhibitory presynaptic ionotropic glutamate receptors and especially mGluRs.[49] However, mGluRs do not seem to be involved, since their antagonists did not affect baseline hippocampal transmission.[50] Moreover, predominantly facilitatory after-effects of intracellular depolarizing pulses[33,35] in the CA1 and CA3 area[5] are difficult to reconcile with the inhibitory presynaptic action of any hypothetical retrograde messenger. The suppression of an inhibitory retrograde messenger is also difficult to reconcile with the observed differences in voltage dependencies between minimal and composite responses, an observation well understandable in the framework of the ephaptic feedback hypothesis.

Another related possibility is that postsynaptic hyperpolarization increases glutamate uptake, thus decreasing its concentration in the synaptic cleft and its suggested presynaptic inhibitory action.[1] However, the above general arguments against participation of a chemical retrograde messenger are applicable to this explanation as well. Although literature data suggest transporters' location in some types of postsynaptic cells,[13] no detectable transporter currents were revealed in CA1 pyramidal neurons.[4] Hyperpolarization effects on presynaptic release have been found in these neurons,[61] without any signs of synaptically activated transporter current when ionotropic glutamate receptors were blocked. If indeed a strong background glutamate release exists, the block of transporter activity should further depress EPSCs. However, glutamate uptake blockers have been found to reduce the size of MF responses only during relatively high-frequency stimulation, when the glutamate release was strongly facilitated, an effect that was entirely reversed by mGluR antagonist.[50] These and related observations on other hippocampal areas[24,56,67] suggest that small and variable glutamate effects on hippocampal responses are mediated by receptor desensitization and only partially by presynaptic inhibition via mGluRs. Our recent observations show that mGluR antagonists do not block the "supralinear" EPSP increase during hyperpolarization (Sokolov *et al*., unpublished observations). Altogether, the literature and our data provide additional evidence against any chemical hypothesis based on either postsynaptic glutamate release or postsynaptic glutamate transporters.

Physiological implications

The existence of the positive ephaptic feedback may explain several phenomena, such as spontaneous synchronous multiquantal releases,[32,62] unusual effects of postsynaptic hyperpolarization on Ca^{2+} responses in a subset of central synapses[14,66] and "all-or-none" responses with a low CV in the visual cortex.[54,57] In fact, one explanation for such "all-or-none" responses is synchronization of transmitter release from several release sites,[57] which can be easily achieved by the ephaptic feedback. The relative number of synaptic inputs with "all-or-none" responses (about 10%) is in striking agreement[57] with an approximate number of large perforated synapses in the visual cortex. The ephaptic feedback may help to understand the physiological significance of the appearance of large ("perforated") synapses following behavioural learning[10] or long-term potentiation induction[16,19,41] (but see Ref. 52). Indeed, the efficacy of such synapses can be larger than that of smaller, non-perforated synapses without spinules, not only due to a larger number of release sites, but also due to the positive intrasynaptic feedback.

The positive feedback was shown here to be fully functional only when a small number of adjacent synapses are synchronously activated or when a synapse is activated together with a large number of electrotonically remote synapses. Thus, the physiological significance of the feedback may essentially consist of amplification of signals from a subset of single synapses. The subset includes synapses which change their size and structure (i.e. acquire spinules and invaginations) as a function of their maturation or activity.[10,16,19,41] The amplification due to the ephaptic feedback can be especially effective for responses induced under natural conditions without voltage clamp at much shorter intervals as compared to the 50-ms interval used in the present study. The facilitating effects of overlapping EPSCs may be of special importance for hippocampal neurons, where bursts of action potentials are commonly observed *in vivo.*

Increasing the number of activated inputs reduces the effects of the positive feedback and would prevent synaptic activity from going beyond a normal physiological limit. When a large amount of similar inputs is activated, additional amplification could be unnecessary or even harmful because of excessive postsynaptic depolarization. The strong diminution of the feedback under conditions when composite EPSCs are induced does not diminish the physiological relevance of the feedback. In fact, simultaneous activation of multiple adjacent inputs commonly used in physiological experiments is expected only infrequently under conditions of natural brain activity. Such activation is characteristic of pathological

(epileptic) states with synchronous discharges of a neuronal population.

CONCLUSIONS

A previous study[61] provided initial evidence in favour of the existence of Byzov's ephaptic feedback[8,9] in central synapses. However, effects of postsynaptic hyperpolarization on indices of transmitter release were found only in a portion of CA1 hippocampal neurons, and contradicted known data on both linear voltage dependence of hippocampal responses and voltage independence of their PPF. In computer simulations, we showed that unusual voltage dependencies should be prominent in large synapses and should be diminished when multiple inputs are activated. These predictions were confirmed experimentally with recordings of both minimal and composite MF EPSCs from the same CA3 neurons. We discussed alternative explanations of our observations and found that the ephaptic feedback hypothesis is the most likely at present. We stress that, independently of underlying mechanisms, our findings of supralinear $A-V$ dependencies and of the effects of the postsynaptic MP shifts on release variables in a subset of central synapses reveal the existence of a novel synaptic mechanism. This mechanism may have important implications in controlling the strength of large synapses by the postsynaptic MP level and by currents generated in adjacent synapses.

Acknowledgements—We thank Drs P. Pakhotin and A. Rossokhin for participation in parts of this work, Drs A. Nistri, M. Volgushev and B. Walmsley for helpful discussions, and W. W. Anderson and Dr A. V. Astrelin for providing computer programs. This work was supported by the Italian Ministero dell'Università e Ricerca Scientifica e Tecnologica, Volkswagen Stiftung, Deutsche Forschungsgemeinschaft, the Russian Foundation for Basic Research and INTAS. N.B. was supported by a NOVARTIS Pharma fellowship.

REFERENCES

1. Arriza J. L., Eliasof S., Kavanaugh M. P. and Amara S. G. (1997) Excitatory amino acid transporter 5, a retinal glutamate transporter coupled to a chloride conductance. *Proc. natn. Acad. Sci. USA* **94,** 4155–4160.
2. Astrelin A. V., Sokolov M. V., Behnisch T., Reymann K. G. and Voronin L. L. (1998) Principal components analysis of minimal excitatory postsynaptic potentials. *J. Neurosci. Meth.* **79,** 169–186.
3. Barrionuevo G., Kelso S. R., Johnston D. and Brown T. H. (1986) Conductance mechanism responsible for long-term potentiation in monosynaptic and isolated excitatory synaptic inputs to hippocampus. *J. Neurophysiol.* **55,** 540–550.
4. Bergles D. E. and Jahr C. E. (1998) Glial contribution to glutamate uptake at Schaffer collateral–commissural synapses in the hippocampus. *J. Neurosci.* **18,** 7709–7716.
5. Berretta N., Rossokhin A. V., Cherubini E., Astrelin A. V and Voronin L. L. (1999) Long-term synaptic changes induced by intracellular tetanization of CA3 pyramidal neurons in hippocampal slices of juvenile rats. *Neuroscience* **92,** 469–477.
6. Berretta N., Rossokhin A. V., Kasyanov A. M., Sokolov M. V., Cherubini E. and Voronin L. L. (2000) Postsynaptic hyperpolarization increases the strength of AMPA mediated synaptic transmission at large synapses between mossy fibers and CA3 pyramidal cells. *Neuropharmacology* **39,** 2288–2301.
7. Bliss T. V. P. and Collingridge G. L. (1993) A synaptic model for memory: long-term potentiation in the hippocampus. *Nature* **361,** 31–39.
8. Byzov A. L. (1968) The component analysis of electro-retinogram in the retina of cold-blooded vertebrates and the regulative function of horizontal cells. Advances in Electrophysiology and Pathology of the Visual System, Veb Georg Thieme, Leipzig.
9. Byzov A. L. and Shura-Bura T. M. (1986) Electrical feedback mechanism in the processing of signals in the outer plexiform layer of the retina. *Vision Res.* **26,** 33–44.
10. Calverley R. K. S. and Jones D. G. (1990) Contributions of dendritic spines and perforated synapses to synaptic plasticity. *Brain Res. Rev.* **15,** 215–249.
11. Claiborne B. J., Amaral D. J. and Cowan W. M. (1986) A light and electron microscopic analysis of the mossy fibers of the rat dentate gyrus. *J. comp. Neurol.* **246,** 435–458.
12. Clark K. A, Randall A. D. and Collingridge G. L. (1994) A comparison of paired-pulse facilitation of AMPA and NMDA receptor-mediated excitatory postsynaptic currents in the hippocampus. *Expl Brain Res.* **104,** 272–278.
13. Danbolt N. C., Chaudhry F. A., Dehnes Y., Lehre K. P., Levy L. M., Ullensvang K. and Storm-Mathisen J. (1998) Properties and localization of glutamate transporters. *Prog. Brain Res.* **116,** 21–41.
14. Denk W., Sugimori M. and Llinas R. (1995) Two types of calcium response limited to single spikes in cerebellar Purkinje cells. *Proc. natn. Acad. Sci. USA* **92,** 8279–8282.
15. Dobrunz L. E., Huang E. P. and Stevens C. F. (1997) Very short-term plasticity in hippocampal synapses. *Proc. natn. Acad. Sci. USA* **94,** 14,843–14,847.
16. Edwards F. A. (1995) Anatomy and electrophysiology of fast central synapses lead to structural model for long-term potentiation. *Physiol. Rev.* **75,** 759–787.
17. Edwards F. A., Konnerth A. and Sakmann B. (1990) Quantal analysis of inhibitory synaptic transmission in the dentate gyrus of rat hippocampal slice: a patch clamp study. *J. Physiol.* **430,** 213–249.
18. Faber D. S. and Korn H. (1989) Electrical field effects: their relevance in central neural networks. *Physiol. Rev.* **69,** 821–863.
19. Geinisman Y., de Toledo-Morell L., Morell F., Heller R. E., Rossi M. and Parshall R. F. (1993) Structural synaptic correlate of long-term potentiation: formation of axospinous synapses with multiple, completely partitioned transmission zones. *Hippocampus* **3,** 435–446.
20. Glitsch M., Llano I. and Marty A. (1996) Glutamate as a candidate retrograde messenger at interneurone–Purkinje cell synapses of rat cerebellum. *J. Physiol.* **497,** 531–537.
21. Hestrin S., Nicoll R. A., Perkel D. J. and Sah P. (1990) Analysis of excitatory synaptic action in pyramidal cells using whole-cell recording from rat hippocampal slices. *J. Physiol.* **422,** 203–225.
22. Hubbard J. I. and Willis W. D. (1962) Hyperpolarization of mammalian motor nerve terminals. *J. Physiol.* **163,** 115–137.
23. Huguenard J. R. (1996) Low-threshold calcium currents in central nervous system neurons. *A. Rev. Physiol.* **58,** 329–348.
24. Isaacson J. S. and Nicoll R. A. (1993) The uptake inhibitor L-*trans*-PDC enhances responses to glutamate but fails to alter the kinetics of excitatory synaptic currents in the hippocampus. *J. Neurophysiol.* **70,** 2187–2191.
25. Jackson J. E. (1991) A User's Guide to Principal Components, John Wiley, New York.
26. Jefferys J. G. R. (1995) Nonsynaptic modulation of neuronal activity in the brain: electric currents and extracellular ions. *Physiol. Rev.* **75,** 689–723.
27. Jonas P., Major G. and Sakmann B. (1993) Quantal components of unitary EPSCs at the mossy fibre synapse on CA3 pyramidal cells of rat hippocampus. *J. Physiol.* **472,** 615–663.
28. Kandel E. R. (1976) Cellular Basis of Behavior, Freeman, San Francisco.
29. Katz B. (1969) The Release of Neural Transmitter Substance, Charles C. Thomas, Springfield, IL.
30. Katz B. and Miledi R. (1967) Tetrodotoxin and neuromuscular transmssion. *Proc. R. Soc. B* **167,** 8–22.
31. Katz B. and Miledi R. (1967) A study of synaptic transmission in the absence of nerve impulses. *J. Physiol.* **192,** 407–436.
32. Korn H., Bausela F., Charpier S. and Faber D. S. (1993) Synaptic noise and multiquantal release at dendritic synapses. *J. Neurophysiol.* **70,** 1249–1254.

33. Kuhnt U., Kleschevnikov A. M. and Voronin L. L. (1994) Long-term enhancement of synaptic transmission in the hippocampus after tetanization of single neurons by short intracellular current pulses. *Neurosci. Res. Commun.* **14,** 115–123.
34. Kullmann D. M. and Nicoll R. A. (1992) Long-term potentiation is associated with increases in quantal content and quantal amplitude. *Nature* **357,** 240–244.
35. Kullmann D. M., Perkel D. J., Manabe T. and Nicoll R. A. (1992) Ca^{2+} entry via postsynaptic voltage-sensitive Ca^{2+} channels can transiently potentiate excitatory synaptic transmission in the hippocampus. *Neuron* **8,** 1175–1183.
36. Liley A. W. (1956) The effects of presynaptic polarization on the spontaneous activity at the mammalian neuromuscular junction. *J. Physiol.* **133,** 427–433.
37. Llinas R., Sugimory M. and Simon S. M. (1982) Transmission by presynaptic spike-like depolarization in the squid giant synapse. *Proc. natn. Acad. Sci. USA* **79,** 2415–2419.
38. Manabe T., Wyllie D. J. A., Perkel D. J. and Nicoll R. A. (1993) Modulation of synaptic transmission and long-term potentiation: effects on paired pulse facilitation and EPSC variance in the CA1 region of the hippocampus. *J. Neurophysiol.* **70,** 1451–1459.
39. Markram H. and Sakmann B. (1994) Calcium transients in dendrites of neocortical neurons evoked by single subthreshold excitatory postsynaptic potentials via low-voltage-activated calcium channels. *Proc. natn. Acad. Sci. USA* **91,** 5207–5211.
40. Maximov V. V. and Byzov A. L. (1996) Horizontal cell dynamics: what are the main factors? *Vision Res.* **36,** 4077–4087.
41. Muller D. (1997) Ultrastructural plasticity of excitatory synapses. *Rev. Neurosci.* **8,** 77–93.
42. Pape H.-C. (1996) Queer current and pacemaker: the hyperpolarization-activated cation current in neurons. *A. Rev. Physiol.* **58,** 299–327.
43. Parnas H., Segel L., Dudel J. and Parnas I. (2000) Autoreceptors, membrane potential and the regulation of transmitter release. *Trends Neurosci.* **23,** 60–68.
44. Perez Velazquez J. L. and Carlen P. L. (2000) Gap junctions, synchrony and seizures. *Trends Neurosci.* **23,** 68–74.
45. Petukhov V. V. and Popov V. L. (1986) Quantitative analysis of ultrastructural changes in synapses of the rat hippocampal field CA3 *in vitro* in different functional states. *Neuroscience* **18,** 823–835.
46. Radpour S. and Thomson A. M. (1991) Coactivation of local circuit NMDA receptor mediated EPSPs induces lasting enhancement of minimal Schaffer collateral EPSPs in slices of rat hippocampus. *Eur. J. Neurosci.* **3,** 602–613.
47. Rudomin P. (1990) Presynaptic inhibition of muscle spindle and tendon organ afferent in the mammalian spinal cord. *Trends Neurosci.* **13,** 499–505.
48. Salin P. A., Scanziani M., Malenka R. C. and Nicoll R. A. (1996) Distinct short-term plasticity at two excitatory synapses in the hippocampus. *Proc. natn. Acad. Sci. USA* **93,** 13,304–13,309.
49. Sanchez-Prieto J., Budd D. C., Herrero I., Vazquez E. and Nicholls D. G. (1996) Presynaptic receptors and the control of glutamate exocytosis. *Trends Neurosci.* **19,** 235–239.
50. Scanziani M., Salin P. A., Vogt K. E., Malenka R. S. and Nicoll R. A. (1997) Use-dependent increases in glutamate concentration activate presynaptic metabotropic glutamate receptors. *Nature* **385,** 630–634.
51. Sokolov M. V., Rossokhin A. V., Behnisch T., Reymann K. G. and Voronin L. L. (1998) Interaction between paired-pulse facilitation and long-term potentiation of minimal EPSPs in rat hippocampal slices: a patch clamp study. *Neuroscience* **85,** 1–13.
52. Sorra K. E., Fiala J. C. and Harris K. M. (1998) Critical assessment of the involvement of perforations, spinules and spine branching in hippocampal synapse formation. *J. comp. Neurol.* **398,** 225–240.
53. Spruston N., Jaffe D. and Johnston D (1994) Dendritic attenuation of synaptic potentials and currents: the role of passive membrane properties. *Trends Neurosci.* **17,** 161–166.
54. Stratford K. J., Tarczy-Hornoch K., Martin K. A., Bannister N. J. and Jack J. J. B. (1996) Excitatory synaptic inputs to spiny stellate cells in cat visual cortex. *Nature* **382,** 258–262.
55. Takeuchi A. and Takeuchi N. (1961) Changes in potassium concentration around motor nerve terminals, produced by current flow, and their effects on neuromuscular transmission. *J. Physiol.* **155,** 46–58.
56. Tong G. and Jahr C. E. (1994) Block of glutamate transporters potentiates postsynaptic excitation. *Neuron* **13,** 1195–1203.
57. Volgushev M., Voronin L. L., Chistiakova M., Artola A. and Singer W. (1995) All-or-none excitatory postsynaptic potentials in the rat visual cortex. *Eur. J. Neurosci.* **7,** 1751–1760.
58. Voronin L. L. (1993) On the quantal analysis of hippocampal long-term potentiation and related phenomena of synaptic plasticity. *Neuroscience* **56,** 275–304.
59. Voronin L. L., Berretta N., Byzov A. L., Gasparini S., Kasyanov A. M., Rossokhin A. V., Sokolov M. V. and Cherubini E. (1999) Postsynaptic hyperpolarization modifies transmitter release at the mossy fibre–CA3 synapse in the hippocampus. *Soc. Neurosci. Abstr.* **25,** 802.
60. Voronin L., Byzov A., Kleschevnikov A., Kozhemyakin M., Kuhnt U. and Volgushev M. (1995) Neurophysiological analysis of long-term potentiation in mammalian brain. *Behav. Brain Res.* **66,** 45–52.
61. Voronin L. L., Volgushev M., Sokolov M., Kasyanov A., Chistiakova M. and Reymann K. G. (1999) Evidence for an ephaptic feedback in cortical synapses: postsynaptic hyperpolarization alters the number of response failures and quantal content. *Neuroscience* **92,** 399–405.
62. Wall M. J. and Usowicz M. M. (1998) Development of the quantal properties of evoked and spontaneous synaptic currents at a brain synapse. *Nature Neurosci.* **1,** 675–683.
63. Wickens J. (1988) Electrically coupled but chemically isolated synapses: dendritic spines and calcium in a rule for synaptic modification. *Prog. Neurobiol.* **31,** 507–528.
64. Winslow J. L., Duffy S. N. and Charlton M. P. (1994) Homosynaptic facilitation of transmitter release in crayfish is not affected by mobile calcium chelators: implications for the residual ionized calcium hypothesis from electrophysiological and computational analyses. *J. Neurophysiol.* **72,** 1769–1793.
65. Wu L.-G. and Saggau P. (1997) Presynaptic inhibition of elicited neurotransmitter release. *Trends Neurosci.* **20,** 204–212.
66. Yuste R., Majewska A., Cash S. S. and Denk W. (1999) Mechanisms of calcium influx into hippocampal spines: heterogeneity among spines, coincidence detection by NMDA receptors, and optical quantal analysis. *J. Neurosci.* **19,** 1976–1987.
67. Zorumski C. F., Mennerick S. and Que J. (1996) Modulation of excitatory synaptic transmission by low concentrations of glutamate in cultured rat hippocampal neurons. *J. Physiol.* **494,** 465–477.
68. Zucker R. S. (1989) Short-term synaptic plasticity. *A. Rev. Neurosci.* **12,** 13–31.

(*Accepted* 15 *June* 2000)